Competition between Hydrogen Fluoride and Hydrogen Chloride Molecular Elimination Channels in the Infrared Multiple-photon Decomposition of 1,2-Dichloro-1,1-difluoroethane

Yo-ichi ISHIKAWA* and Shigeyoshi ARAI
The Institute of Physical and Chemical Research, Wako, Saitama 351
(Received August 25, 1983)

Time-resolved infrared emission spectra have been measured in the infrared multiple-photon decomposition of $CClF_2CH_2Cl$. The spectra were composed of emissions attributable to vibrationally excited HF* and HCl*. The emission yield of HF* increased rapidly with an increase in the fluence, while the yield of HCl* showed a maximum at 20 J cm^{-2}. These results suggest that the HF and HCl molecular elimination channels compete with each other in the unimolecular decomposition of highly vibrationally excited parent molecules. The stochastic trajectory calculations provided a satisfactory description of the fluence dependences of the HF and HCl yields observed here for $CClF_2CH_2Cl$ and previously for CHClFCHClF.

The infrared multiple-photon decomposition (IRMPD) of large molecules frequently shows more than one reaction channel, leading to a variety of products.[1] For the occurrence of a particular reaction channel, the parent molecules must be excited to levels above the threshold energy of the corresponding channel in the multiple-photon excitation process. The branching ratio among the channels can be interpreted in terms of the distribution of excited molecules with respect to the internal energy and the kinetic parameters of excited molecules as a function of the internal energy. Although there are several quantitative methods of determining product yields in the IRMPD of large molecules, the energy distribution and kinetic parameters have been studied to only a limited extent.

The effects of the laser fluence (J cm^{-2}) and the intensity (W cm^{-2}) on the IRMPD of large molecules have been reported extensively in recent publications.[1,2] It is generally accepted that an increase in the fluence significantly increases product yields, while, in contrast, a change in the intensity slightly affects the IRMPD. However, the laser intensity is directly proportional to the rates of optical absorption and stimulated emission for molecules in an intense laser field. The energy distribution should depend on the rates of these optical processes as well as on the rates of the decomposition of excited molecules.

West *et al.* have investigated the fluence dependences of HF and HCl molecular elimination channels in the IRMPD of $CClF_2CH_3$ using an infrared emission spectroscopic technique.[3] Krajnovich *et al.* have studied the fluence dependences of Cl atomic elimination and C–C bond rupture in the IRMPD of C_2F_5Cl by the use of a molecular-beam technique.[4] These experiments have, in principle, two advantages. One is that there is no complication caused by the subsequent reactions of initial intermediate products; another is that the fluence variation within the reaction zone is relatively small. Since IRMPD usually requires high fluences, the laser beam is tightly focussed in a reaction cell. Therefore, the resulting inhomogeneity of the fluence must be considered carefully in the analysis of the data. In infrared-emission and molecular-beam experiments, it is possible to detect emitting species and fragment species produced in a small reaction zone, where the fluence variation is somewhat limited.

In this study we have examined the IRMPD of $CClF_2CH_2Cl$ using a time-resolved infrared-emission spectroscopic technique. The experimental results show that HF and HCl molecular-elimination reactions occur competitively in the decomposition of highly vibrationally excited parent molecules. In addition, the fluence dependences of the channels are quite different from each other. These findings are similar to those obtained with the IRMPD of CHClFCHClF in a previous study.[5] The stochastic trajectory calculations can satisfactorily explain the observed fluence dependences in both studies on a reasonable assumption of kinetic parameters.

Experimental

The experimental apparatus used here is essentially the same as in a previous study.[6] The details have been described elsewhere.[7] The pulsed beam from a Lumonics TEA 103 CO_2 laser was truncated by an iris with a diameter of 9.9 mm and focussed in an irradiation cell by means of a BaF_2 lens with a focal length of 20 cm. The pulse profile was a spike of 80-ns fwhm without any tail. The laser was tuned to the R(20) line of the 9.6-μm CO_2 band at 1078.59 cm^{-1} and operated at a repetition rate of 0.7 Hz. The intensity distribution across the laser beam after passing through the iris was nearly flat; the deviation from the mean value was less than 15%. The beam area at focus was estimated to be 5×10^{-3} cm^2 from the beam divergence of 2 mrad. The laser fluence at focus was calculated from the beam area and the laser energy. The length of the reaction zone inside the cell was 2 cm along the laser beam, and the focal point was in the middle. The fluence at each end was estimated to be 60% of that at focus. In addition, the optical system was arranged so that the emission at focus could be monitored most efficiently during the observation. An InSb detector was set behind the exit slit of a Ritsu Kogaku MC-20L monochromator. Raw signals from the detector were first amplified by means of a PAR model 115 preamplifier. Then, the amplified signals were treated with a PAR model 162 boxcar averager and PAR model 155 gated integrator for the spectrum measurements, and with a Biomation 8100 transient digitizer and Keisoku Giken model 8100 signal averager for the time-resolved intensity measurements. The aperture duration, τ_g, and the aperture delay, τ_d, used for the boxcar averager were 10 and 3 μs respectively. The laser pulse picked up with a photon-drag detector (Hamamatsu TV, model B749) was used as a trigger signal of the detection system. The overall rise time was about 2 μs.

The flow rate of a reactant gas in the cell was 10 Torr

$cm^3\,min^{-1}$ (1 Torr≈133.3 Pa),[8] and the pressure was measured with a MKS Baratron model 220 BH manometer (10 Torr pressure range). The reactant gas, $CClF_2CH_2Cl$, was purchased from PCR Research Chemicals and was purified by trap-to-trap distillation before use.

Results and Discussion

First of all, the final products in the IRMPD of $CClF_2CH_2Cl$ were examined using infrared-absorption spectroscopic analysis. A special cell with a KBr window at each end (10 cm in length and 1.5 cm in inner diameter) was filled with 5-Torr $CClF_2CH_2Cl$. The laser beam was tightly focussed by means of a 7.5-cm focal length BaF_2 lens. The pulse energy and the focus fluence were 0.20 J and 280 J cm^{-2} respectively. The infrared-absorption spectrum was measured after irradiation using a JASCO type A-102 infrared spectrometer. The products assigned in the infrared spectrum are HCl (ν_1=2900 cm^{-1}), SiF_4 (ν=1030 cm^{-1}),[9] CF_2CHCl (ν_1=3130 cm^{-1}; ν_2=1740 cm^{-1}; ν_3=1330 cm^{-1}; ν_4=1200 cm^{-1}; ν_5=970 cm^{-1}),[10] and CClFCHCl (ν_3 for cis- and/or trans-form=1650 cm^{-1}; ν_6 for trans-form=850 cm^{-1}).[11] The formation of SiF_4 is explained by the secondary reaction of the primary product, HF, with the glass wall. These products suggest that the α,β-molecular elimination of HF and HCl occurs in the IRMPD of $CClF_2CH_2Cl$:

$$CClF_2CH_2Cl + mh\nu \rightarrow CF_2CHCl + HCl, \quad (1)$$

and:

$$CClF_2CH_2Cl + nh\nu \rightarrow CClFCHCl + HF. \quad (2)$$

Figure 1 presents the fluence effects on the infrared emission spectra for 1-Torr $CClF_2CH_2Cl$ irradiated at 1078.59 cm^{-1} in a flow system. The fluences at focus are indicated in the same figure. The slit function, with 0.056 μm fwhm, is also illustrated at the top of the figure. The emission with two peaks in the wavelength region from 3.1 to 4.2 μm is due to highly vibrationally excited HCl*, while the emission in the region from 2.2 to 3.1 μm is due to HF*. The spectral simulation based on the spectroscopic constants of HCl and HF supports the above assignments.[5,6] We could not detect any meaningful emission in the same wavelength region when the empty cell was irradiated at a fluence of 53 J cm^{-2}, as is shown in Fig. 1f. Since all the spectra have been measured under the same conditions except for the fluence, the intensities of the HF* and HCl* emissions can be said to be proportional to the yields of HF* and HCl* respectively among the spectra. As the fluence is increased, the intensity of HF*(I_{HF*}) grows much more rapidly than the intensity of HCl*(I_{HCl*}). The ratio of I_{HF*} to I_{HCl*} changes from 0.4 at 11 J cm^{-2} to 2.5 at 43 J cm^{-2}, where HF* and HCl* emission intensities are monitored at the wavelengths of about 2.8 and 3.8 μm respectively.

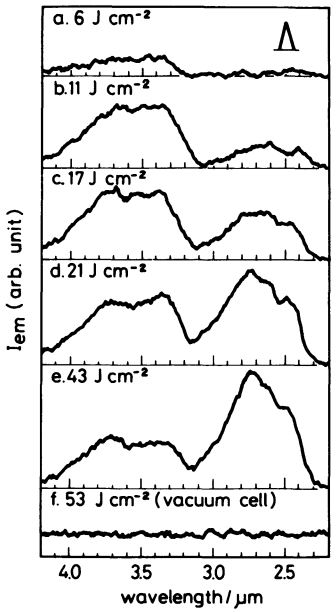

Fig. 1. Infrared fluorescence spectra observed for 1-Torr $CClF_2$-CH_2Cl irradiated with CO_2 TEA laser. Laser wavenumber, 1078.59 cm^{-1}.

Setser and his co-workers have examined the HF(DF) and HCl(DCl) elimination reactions of highly vibrationally excited haloethanes prepared in radical combination reactions.[12,13] They estimated that α,α-elimination contributes approximately 10% to the total molecular elimination in CHF_2CH_3. We have measured the fluorescence spectrum in the IRMPD of $CHCl_2CF_3$, where the α,α- and α,β-elimination channels were expected to give HCl* and HF* respectively. There appears to be no contribution of HCl* emission to the observed spectrum in Fig. 2. These facts suggest that α,α-elimination is a minor process in the decomposition of vibrationallly excited haloethanes.

Figure 3 presents the time dependences of the emission intensities observed at 2.4, 2.8, 3.0, 3.4, and 3.8 μm for 1-Torr $CClF_2CH_2Cl$. The fluence was 29 J cm^{-2}. The spectrum simulation suggests that the emission at 2.4 μm mainly corresponds to the R-branch of the HF* (v'=1)→HF(v''=0) transition, and those at 2.8 and 3.0 μm, to several transitions (Δv=1) originating from HF* at various vibrational levels. Similarly, the emissions at 3.4 and 3.8 μm are due to several transitions (Δv=1) of vibrationally excited HCl*. The emission profiles show a rapid initial rise and then a rapid

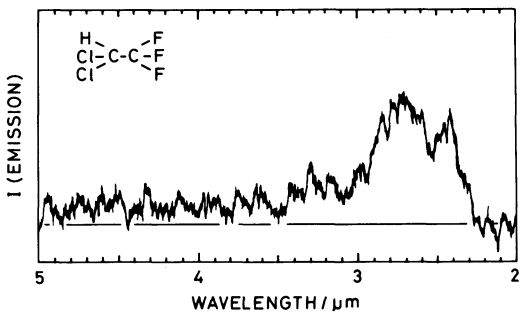

Fig. 2. Infrared fluorescence spectra observed for 5-Torr $CHCl_2CF_3$ irradiated with CO_2 TEA laser. Laser wavenumber, 1078.59 cm^{-1}; fluence, 40 J cm^{-2}; wavelength resolution, 0.068 μm fwhm.

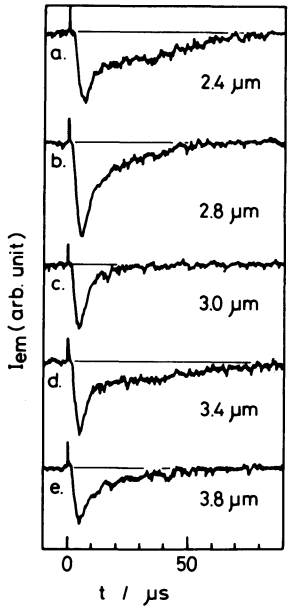

Fig. 3. Typical HF* and HCl* fluoresence signals observed for 1.0-Torr $CClF_2CH_2Cl$. Laser fluence, 29 J cm^{-2}; emission measurement wavelength, 3.8 and 3.4 μm for HCl* and 3.0, 2.8, and 2.4 μm for HF*; wavelength resolution, 0.056 μm fwhm; laser wavenumber, 1078.59 cm^{-1}.

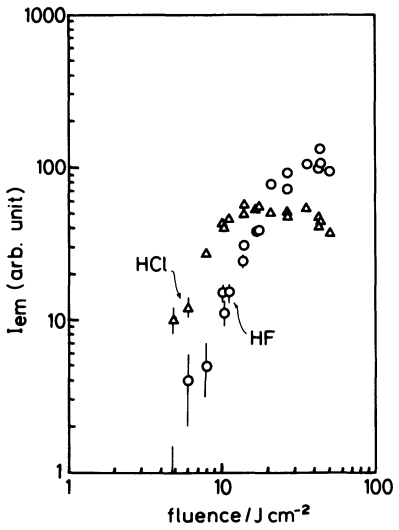

Fig. 4. Peak emission intensities of HCl* (triangles, at 3.8 μm) and HF* (circles, at 2.8 μm) *vs.* laser fluence observed for IRMPD of $CClF_2CH_2Cl$. Laser wavenumber, 1078.59 cm^{-1}.

decay, followed by a slower decay. Although the slow-decay component is relatively small in the emission at 3.0 μm, there is no essential difference in dynamic behavior between the two emitting species, HF* and HCl*. Both may be produced by a similar process, *i.e.*, molecular elimination from highly vibrationally excited $CClF_2CH_2Cl$*. The considerably different fluence dependences observed for HF* and HCl* seem to exclude the possibility that the initial molecular elimination to form HCl* and $CHClCF_2$ is followed by the subsequent elimination of HF* from $CHClCF_2$.

The rate constants for the quenching of vibrationally excited HF* and HCl* by some simple molecules have been determined in laser-induced infrared fluorescence experiments.[14,15] On the assumption that the quenching-rate constants of HF* and HCl* by $CClF_2CH_2Cl$ are approximately the same as those by CH_4, the lifetimes of HF* and HCl* are estimated to be a few microseconds in 1-Torr $CClF_2CH_2Cl$. Since these lifetimes are much shorter than the spontaneous fluorescence lifetimes of HF* and HCl*,[16] these excited molecules can be said to be mainly deactivated in collisions. We propose that large fractions of HF* and HCl* are produced during the laser pulse by means of Reactions 1 and 2. These fractions are responsible for the initial emission spikes in Fig. 3. The rise time of the spike corresponds to the response time of the detection system, while the rapid decay is due to the collisional deactivation of HF* and HCl*. On the other hand, HF* and HCl* are also produced in the collision-induced excitation of $CClF_2CH_2Cl$, followed by immediate decomposition:

$$CClF_2CH_2Cl'' + CClF_2CH_2Cl'' \rightarrow CClF_2CH_2Cl^{\dagger} + CClF_2CH_2Cl', \quad (3)$$

and:

$$CClF_2CH_2Cl^{\dagger} \rightarrow CF_2CHCl + HCl^* \rightarrow CClFCHCl + HF^*, \quad (4)$$

where $CClF_2CH_2Cl^{\dagger}$ represents a reactant molecule excited to a level beyond the decomposition threshold. $CClF_2CH_2Cl''$ is excited below or just above the threshold. Its lifetime is as long as several dozen microseconds. $CClF_2CH_2Cl'$ is a deactivated molecule. The collision-induced processes cause a delayed fluorescences of HF* and HCl* lasting for about 80 μs.

The emission intensities of HF* and HCl* are plotted against the laser fluence in Fig. 4, where I_{HF^*} and I_{HCl^*} are measured at 2.8 and 3.8 μm respectively. The Einstein coefficient of HF* is about five times larger than that of HCl*.[17] Therefore, I_{HF^*} divided by a factor of five and I_{HCl^*} are proportional to the yields of HF* and HCl* on the same scale, if the quenching rate of HF* is equal to that of HCl*. West *et al.* have measured the fluence dependences of the HF* and HCl* emission intensities in the IRMPD of $CClF_2CH_3$.[3] In their measurements, both intensities were found to increase almost linearly with an increase in the fluence. They reported that the calculated RRKM curves for k(HF) and k(HCl) *vs.* the internal energy are virtually parallel over a wide range. This result leads to the constant HF*/HCl* ratio in the corresponding range. In our study of $CClF_2CH_2Cl$, however, the HF*/HCl* ratio clearly depends on the laser fluence. The emission due to HCl* is much stronger than that due to HF* at lower fluences, while I_{HF^*}/I_{HCl^*} is about three at 50 J cm^{-2}. This fact suggests that highly vibrationally excited $CClF_2CH_2Cl$ decomposes competitively *via* HF and HCl molecular-elimination channels and that the branching ratio changes depending on the internal energy of the excited parent molecule. We also observed similar fluence dependences of I_{HF^*} and I_{HCl^*} for a mixture of 0.2-Torr $CClF_2CH_2Cl$ and 4-Torr Ar when

it was irradiated in the fluence region from 30 to 43 J cm^{-2}. Krajnovich *et al.* have examined the IRMPD of C_2F_5Cl in a molecular beam. Cl atomic elimination was dominant at lower fluences. As the fluence was increased, however, the atomic elimination approached saturation, and the C–C bond scission became more eminent.[4] The fluence dependences seem to be consistent with the present study.

The infrared fluorescence experiment can not provide any information concerning the production of HF and HCl in a ground vibrational state. In comparing the observed results with the calculated ones, we assume that the emission intensities of HF* and HCl* are proportional to the total yields of HF and HCl respectively. We simply use the peak emission intensities monitored at 2.8 and 3.8 μm in place of the integrated emission intensities, because a change in fluence does not appreciably affect the shapes of the fluorescence spectra due to HF* and HCl*. It is extremely difficult to separate the HF* and HCl* produced directly in the IRMPD from those produced in collision-induced processes. Therefore, I_{HF^*} and I_{HCl^*} probably correspond to the emissions of HF* and HCl* arising from the IRMPD, not only within the laser pulse, but also after the pulse.

Barker proposed an exact stochastic method based on an energy-grained master equation for the theoretical interpretation of IRMPD.[18] The method has been further applied to consecutive and competitive IRMPD.[19] The details will not be given here. Although there has been no kinetic or thermodynamic study of the two elimination channels of $CClF_2CH_2Cl$ itself, the Arrhenius parameters of HF and HCl elimination reactions have been reported on a number of halogenated hydrocarbons: log A=13—14 and E_0=55—70 kcal mol^{-1} (1 cal=4.184 J) for HF elimination; log A=11—14 and E_0=50—60 kcal mol^{-1} for HCl elimination.[20] The numerical values and assumptions employed for the present calculations are as follows: (a) σ_0 (infrared absorption cross-section of $CClF_2CH_2Cl$ in a ground vibrational state)=1.3×10^{-19} cm^2; (b) the fundamental vibrational frequencies of the $-CH_2Cl$ group in the CH_3CH_2Cl and the $-CClF_2$ group in CF_3CClF_2[21] were used for those of the $-CH_2Cl$ and $-CClF_2$ groups in $CClF_2CH_2Cl$; (c) the laser pulse was assumed to have a 80-ns duration and a constant intensity; (d) parent molecules excited to levels higher than threshold energies were assumed to undergo competitively three processes: collisional deactivation ($k_d=1\times10^6$ s^{-1}), HF elimination, and HCl elimination. The cross-section was determined from the absorption measurement at 1078.59 cm^{-1}. The fundamental vibration frequencies are tabulated in Table 1. The weights of the three reaction processes depend on their rates. The number of trajectories is 1000 in the present calculation.

The simulation of the fluence dependences shown in Fig. 4 was performed for various Arrhenius parameters of the two reaction channels. The absorption cross-section was assumed to have the following form with respect to a given energy level n: $\sigma_n=\sigma_0/(n+1)^\alpha$, where α can be regarded as a parameter. The following set of numerical values gave the best-fitting simulation: log A=12 and E_0=50 kcal mol^{-1} for HCl elimination; log A=14 and E_0=68 kcal mol^{-1} for HF elimination; α=0.2. Table 2 shows the calculated results of the IRMPD of $CClF_2CH_2Cl$ at various fluences using the above-mentioned parameters. The decomposition within the laser pulse becomes more important with an increase in the fluence. In the intermediate fluence region of 10—20 J cm^{-2}, however, the decomposition after the end of the pulse contributes significantly to the total production of HCl,[23] where HCl elimination has a lower threshold energy. The typical energy distributions $P(n)$, *i.e.*, the fraction of molecules at a given energy level n, are illustrated in Fig. 5, where $CClF_2CH_2Cl$ is supposed to be irradiated at six different fluences. The cross-hatched and filled areas correspond to the fractions of the HCl (F_{total}(HCl)) and HF(F_{total}(HF)) elimination channels respectively in the figure. As the degree of vibration freedom s is as large as 18 in $CClF_2CH_2Cl$, the unimolecular decomposition rates calculated for molecules at levels a little higher than the threshold energies, *i.e.*, n=17—23 for HCl elimination and n=23—27 for HF elimination, are smaller than the assumed quenching rate. The k_{HCl} (n) and k_{HF} (n) are about equal to the quenching rate k_d at n=24 and 28 respectively. The two rate constants are roughly equal to each other at n=35; the value is 2.0×10^8 s^{-1}. When the laser fluence is 20 J cm^{-2}, the absorption rate for the molecule at n=50 is five times less than k_{HCl} and 30 times less than k_{HF}. Therefore, it is hard to excite molecules to such high energy levels.

The calculated fluence dependences of the HCl elimination and HF elimination are shown in Fig. 6, where the decomposition after the end of the pulse

Table 1. Fundamental vibration frequencies of $CClF_2CH_2Cl$ and CHClFCHClF used in the calculations

$CClF_2CH_2Cl$		CHClFCHClF	
Vibration[a]	Frequency ν/cm^{-1}	Vibration[a]	Frequency ν/cm^{-1}
CH_2 a-stretch.	3000	CH a-stretch.	2983
CH_2 s-stretch.	3000	CH s-stretch.	2850
CH_2 scis.	1430	CH op-bend.	1439
CH_2 wag.	1300		1357
CH_2 twist.	1240	CH ip-bend.	1297
CF_2 a-stretch.	1185		1239
CF_2 s-stretch.	1110	CF a-stretch.	1188
CC stretch.	1030	CF s-stretch.	1105
CH_2 rock.	820	CC stretch.	1032
CCl a-stretch.	770	CCl a-stretch.	794
CCl s-stretch.	660	CCl s-stretch.	753
CF_2Cl deform.	454	CFCl a-deform.	700
CF_2Cl deform.	441	CFCl s-deform.	628
CCCl a-deform.	336	CCFCl deform.	462
CCCl s-deform.	330		452
CF_2Cl deform.	315		236
Torsion.	251		236
CF_2Cl deform.	186	Torsion.	160

a) See Ref. 22 for abbreviation.

TABLE 2. IRMPD OF $CClF_2CH_2Cl$

ϕ / J cm^{-2}	$\bar{n}$[a]	n[b]	Within pulse			After pulse		Total R[f]	P[g]
			F(HCl)[c]	F(HF)[c]	R[d]	F(HCl)[e]	F(HF)[e]		
4	12.7	17.2	0.001	0	—	0.002	0	—	0.003
6	16.8	24.4	0	0	—	0.058	0.001	58	0.059
8	19.9	31.0	0.025	0.003	8.3	0.180	0.006	22.8	0.214
10	23.1	37.2	0.062	0.018	4.8	0.348	0.022	10.3	0.451
12	25.4	42.6	0.167	0.052	3.2	0.375	0.029	6.7	0.423
14	27.5	47.0	0.283	0.109	2.6	0.332	0.036	4.2	0.760
16	29.1	51.2	0.367	0.156	2.4	0.286	0.038	3.4	0.846
18	30.3	54.0	0.462	0.209	2.2	0.204	0.034	2.7	0.909
20	31.1	55.8	0.531	0.241	2.2	0.151	0.024	2.6	0.947
25	32.5	59.7	0.589	0.318	1.9	0.062	0.013	2.0	0.982
30	33.2	62.0	0.618	0.342	1.8	0.024	0.007	1.8	0.991
35	33.6	62.9	0.607	0.382	1.6	0.008	0.002	1.6	0.999
40	33.9	63.5	0.578	0.417	1.4	0.004	0.001	1.4	1.0
45	34.1	64.8	0.588	0.409	1.4	0.002	0	1.4	1.0
50	34.5	65.6	0.556	0.444	1.3	0	0	1.3	1.0
55	34.6	66.0	0.537	0.463	1.2	0	0	1.2	1.0
60	34.8	66.0	0.543	0.457	1.2	0	0	1.2	1.0
65	34.9	66.3	0.516	0.484	1.1	0	0	1.1	1.0
70	35.2	66.4	0.530	0.470	1.1	0	0	1.1	1.0

a) Average number of photons contained in a molecule at end of laser pulse. b) Average number of photons absorbed per molecule at end of laser pulse. c) Fraction of reaction within laser pulse. d) F(HCl)/F(HF). e) Fraction of reaction after pulse. f) F(HCl)/F(HF), where collisions are taken into consideration. g) Reaction probability.

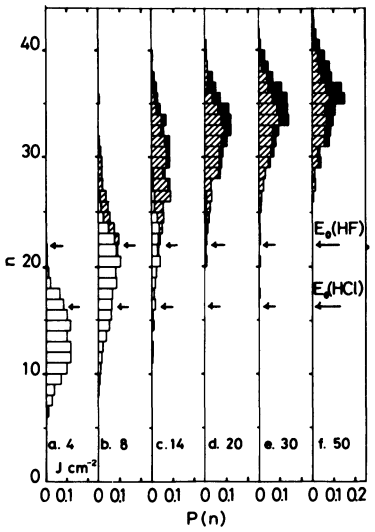

Fig. 5. Typical vibrational population distributions for $CClF_2CH_2Cl$ irradiated at various fluences. Cross-hatched and filled areas indicate the extents of HCl and HF elimination reactions, respectively. $\sigma_n=\sigma_0/(n+1)^{0.2}$ cm^2. The postirradiation decomposition was taken into consideration.

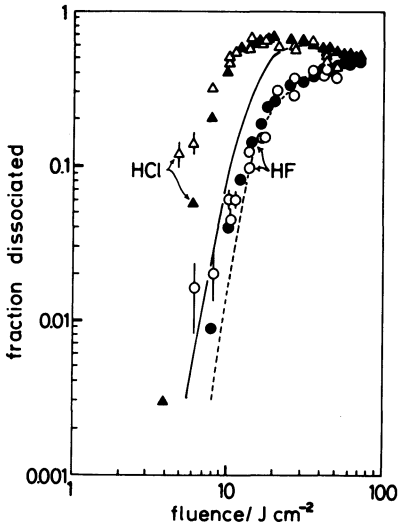

Fig. 6. Comparison of calculated yields of HCl and HF to observed ones in IRMPD of 1-Torr $CClF_2CH_2Cl$ at various fluences. Filled triangles, calculated yields of HCl; triangles, observed yields of HCl; filled circles, calculated yields of HF; circles, observed yields of HF. Solid and dotted curves show the calculated fractions of HF and HCl produced within the pulse.

has been taken into consideration. The filled triangles and filled circles present F_{total}(HCl) and F_{total}(HF) respectively. The same figure also shows the fluence dependences of the observed I_{HCl^*} (open triangles) and I_{HF^*} (open circles) values, where the scales have been chosen arbitrarily so that the experimental data fit the calculated ones. The I_{HF^*}/F_{total} (HF) ratio was found to be approximately three times larger than the I_{HCl^*}/F_{total} (HCl) ratio. From the emission efficiencies of HCl* and HF*, the factor can be expected to be five if these molecules are in the $v'=1$ state.[17] The solid and dotted curves in Fig. 6 present the fractions of HCl and HF respectively which are produced within the pulse.

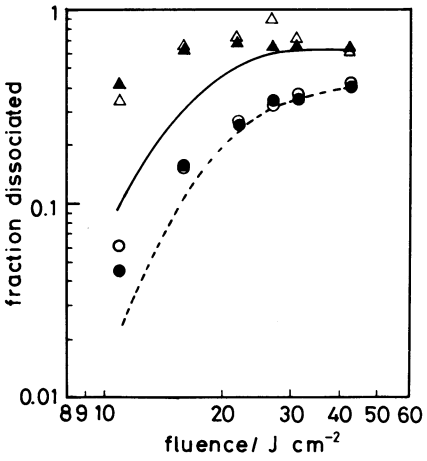

Fig. 7. Comparison of calculated yields of HCl and HF to observed ones in IRMPD of 2-Torr CHClFCHClF at various fluences. Filled triangles, calculated yields of HCl; triangles, observed yields of HCl; filled circles, calculated yields of HF; circles, observed yields of HF. Solid and dotted curves show the calculated fractions of HF and HCl produced within the pulse.

Our previous paper has reported the fluence dependences of I_{HF^*} and I_{HCl^*} in the IRMPD of CHClFCHClF using the same experimental technique.[5] By applying the stochastic trajectory calculation to the compound, we obtained the results in Fig. 7. The fundamental vibration frequencies are also tabulated in Table 1. The kinetic parameters for the HF and HCl elimination reactions are the same as $CClF_2CH_2Cl$. The α parameter is changed into 0.3, which seems to give a better fit. I_{HF^*}/F_{total} (HF) is four times larger than I_{HCl^*}/F_{total} (HCl).

At present, the calculations seems to have a somewhat unavoidable uncertainty because of the lack of the kinetic parameters of $CClF_2CH_2Cl$ and CHClFCHClF, together with incomplete understanding of the multiple-photon absorption process. However, the calculated results satisfactorily describe the fluence dependences of I_{HF^*} and I_{HCl^*} for the IRMPD of $CClF_2CH_2Cl$ and CHClFCHClF. It is interesting that the IRMPD is able to induce the reaction channel with a higher threshold energy, rather than the channel with the lowest threshold energy, under some selected experimental conditions.

The authors wish to express their thanks to Miss Kyoko Sugita for the computer calculations. They also wish to express their thanks to Dr. Takashi Igarashi for the assignments of the fundamental vibration frequencies of haloethanes.

References

1) W. C. Danen and J. C. Jang, "Multiphoton Infrared Excitation and Reaction of Organic Compounds," in "Laser-Induced Chemical Processes," ed by J. I. Steinfeld, Plenum Press, New York (1981), Chap. 2, p. 63.
2) J. B. Black, P. Kolodner, M. J. Shultz, E. Yablonovitch, and N. Bloembergen, *Phys. Rev., A*, **19**, 704 (1979); J. C. Stephenson and D. S. King, *J. Chem. Phys.*, **78**, 186 (1983).
3) G. A. West, R. E. Weston, Jr., and G. W. Flynn, *Chem. Phys.*, **35**, 275 (1978).
4) D. J. Krajnovich, A. Giardini-Guidoni, Aa. S. Sudbo, P. A. Schultz, Y. R. Shen, and Y. T. Lee, "Crossed Laser and Molecular Beam Study of Multiphoton Dissociation of C_2F_5Cl," in "Laser-Induced Processes in Molecules," ed by K. L. Kompa and S. D. Smith, Springer-Verlag, Berlin (1979), p. 176.
5) Y. Ishikawa and S. Arai, *Chem. Phys. Lett.*, **103**, 68 (1983).
6) C. R. Quick, Jr., and C. Wittig, *J. Chem. Phys.*, **72**, 1694 (1980).
7) Y. Ishikawa, T. Yamazaki, Y. Hama, and S. Arai, *Appl. Phys., B*, **32**, 85 (1983).
8) No change could be observed in the ratio of I_{HCl^*} to I_{HF^*}, even at a fast flow rate of 200 Torr cm^3 min^{-1}. This fact indicates that the secondary reactions involving stable products, $CClF_2CH_2Cl^*+HCl(HF)\rightarrow CClF_2CH_2Cl+HCl^*(HF^*)$ and $CF_2CHCl+nh\nu\rightarrow CFCCl+HF^*$, do not occur appreciably at the slow flow rate, *i.e.*, 10 Torr cm^3 min^{-1}, used here.
9) E. A. Jones, J. S. Kirby-Smith, P. L. H. Woltz, and A. H. Nielsen, *J. Chem. Phys.*, **19**, 242 (1950).
10) J. R. Nielsen, C. Y. Liang, and D. C. Smith, *J. Chem. Phys.*, **20**, 1090 (1952).
11) N. C. Craig, G. Y. Lo, C. D. Needham, and J. Overend, *J. Am. Chem. Soc.*, **86**, 3232 (1964).
12) K. C. Kim and D. W. Setser, *J. Phys. Chem.*, **76**, 283 (1972).
13) K. C. Kim, D. W. Setser, and B. E. Holmes, *J. Phys. Chem.*, **77**, 725 (1973).
14) H. L. Chen and C. B. Moore, *J. Chem. Phys.*, **54**, 4080 (1971).
15) J. K. Hancock and W. H. Green, *J. Chem. Phys.*, **59**, 6350 (1973).
16) J. T. Yardley, "Introduction to Molecular Energy Transfer," Academic Press, New York (1980), p. 58.
17) J. M. Herbelin and G. Emanuel, *J. Chem. Phys.*, **60**, 689 (1974).
18) J. R. Barker, *J. Chem. Phys.*, **72**, 3686 (1980).
19) R. E. Weston, Jr., *J. Phys. Chem.*, **86**, 4864 (1982).
20) P. J. Robinson and K. A. Holbrook, "Unimolecular Reactions," Wiley-Interscience, London (1972), p. 221.
21) J. R. Nielsen, C. Y. Liang, R. M. Smith, and D. C. Smith, *J. Chem. Phys.*, **21**, 383 (1953).
22) T. Shimanouchi, "Tables of Molecular Vibrational Frequencies," NSRDS-NBS, 39 (1972), Consolidated Vol. 1, p. 104.
23) Y. Ishikawa, H. Kasugai, T. Ishii, and S. Arai, to be published.